Numerical Verification of Bounce-Harmonic Resonances in Neoclassical Toroidal Viscosity for Tokamaks

Kimin Kim,[1,*] Jong-Kyu Park,[1] and Allen H. Boozer[2]
[1]*Princeton Plasma Physics Laboratory, Princeton, New Jersey 08543, USA*
[2]*Department of Applied Physics and Applied Mathematics, Columbia University, New York, New York 10027, USA*
(Received 16 November 2012; published 2 May 2013)

This Letter presents the first numerical verification for the bounce-harmonic (BH) resonance phenomena of the neoclassical transport in a tokamak perturbed by nonaxisymmetric magnetic fields. The BH resonances were predicted by analytic theories of neoclassical toroidal viscosity (NTV), as the parallel and perpendicular drift motions can be resonant and result in a great enhancement of the radial momentum transport. A new drift-kinetic δf guiding-center particle code, POCA, clearly verified that the perpendicular drift motions can reduce the transport by phase-mixing, but in the BH resonances the motions can form closed orbits and particles radially drift out fast. The POCA calculations on resulting NTV torque are largely consistent with analytic calculations, and show that the BH resonances can easily dominate the NTV torque when a plasma rotates in the perturbed tokamak and therefore, is a critical physics for predicting the rotation and stability in the International Thermonuclear Experimental Reactor.

DOI: 10.1103/PhysRevLett.110.185004 PACS numbers: 52.55.Fa, 52.65.Vv

Tokamaks are highly sensitive to nonaxisymmetric magnetic fields, which can be generated by intrinsic error fields, magnetohydrodynamic activities, and/or externally applied magnetic perturbations. It has been well known that even a small magnetic perturbation of order of $|\delta B/B| \sim 10^{-4}$ can dramatically modify tokamak transport and thereby various macroscopic stabilities such as locked modes, edge localized modes, and resistive wall modes [1–4].

One of the important effects caused by the nonaxisymmetric magnetic perturbations is the modification of the radial transport of toroidal momentum. This has been called neoclassical toroidal viscosity (NTV), as the toroidal rotation can be largely damped or changed with the toroidal symmetry-breaking magnetic perturbations. The toroidal rotation changes associated with the NTV have been well accepted in theory [5–7], and also widely observed in experiments with magnetic perturbations in various devices such as NSTX [8–10] and DIII-D [11,12]. The toroidal rotation is an important parameter to determine the tokamak stability, from the macroscopic to the microscopic scale, and thus, scientific interests on the NTV and the control of the toroidal rotation through the NTV have been rapidly increased.

The NTV physics is featured by complicated parametric dependencies. The collisionality is one of critical parameters, as is well known by the $1/\nu$ regime [13] in the relatively high collisionality and the $\nu_-\sqrt{\nu}$ regime [14] with the very low collisionality. The $\vec{E} \times \vec{B}$ precession drift is another dominant parameter [15], as the very low $\vec{E} \times \vec{B}$ precession rate ω_E can lead to the superbanana plateau regime [16]. Analytic treatments have been quite successful in capturing the essential physics in these regimes, but in practice, the connection among different regimes is required to make a prediction in tokamaks, which are almost always composed of multiple regimes across the volume [17,18].

There is an important missing component, however, in the connection between each analytic treatment for each regime, the bounce-harmonic (BH) resonance. The BH resonance was predicted first by Linsker and Boozer [19] and Mynick [20] and reformulated by Park [17] as essential physics to determine the NTV transport unless ω_E is extremely low, but has never been verified by experiments or numerical simulations so far. The BH resonances occur when the parallel bounce motions are resonant with the perpendicular $\vec{E} \times \vec{B}$ motions. That is, when the precession rate ω_E is comparable to the bounce frequency ω_b, the particles can return back to the same turning point after a few or a number of toroidal rotations, i.e., $\ell\omega_b \sim n\omega_E$ where ℓ is the digit representing the bouncing class of particles [17] and n is the toroidal mode number of perturbations. Since there are almost always a small number of particles that satisfy the $\ell\omega_b \sim n\omega_E$ condition in a Maxwellian distribution, the BH resonances change the NTV prediction. Also note that it is the only mechanism to enhance the NTV transport in the high ω_E.

The physics of the BH resonances was rather clear by theory, but the simplified collisionality to connect all the regimes including the BH resonances requires a serious numerical verification using the realistic collisional operator. Modification of particle orbit and transport by nonaxisymmetric fields are essential in NTV physics; thus, particle simulation has the benefit of studying the BH resonance as well as fundamental NTV physics. Indeed, this simulation gives a new finding of orbit evolutions of charged particles confined in magnetic field by electric field and its resonance with parallel and perpendicular

motion of particles. This Letter shows a new type of bounce orbit created by BH resonances and provides the first successful verification of the BH resonances in NTV using a new drift-kinetic δf guiding-center particle code.

The new code, POCA (Particle Orbit Code for Anisotropic pressures), has been successfully developed and shows various essential NTV features, such as the quadratic δB dependency, the $1/\nu$ and $\nu_-\sqrt{\nu}$ behaviors including the superbanana plateau, qualitatively and quantitatively in the zero ω_E limit [21]. As will be briefly introduced later, the POCA simulation precisely follows the guiding-center orbits without approximations such as the regime separation, the limitation on trapped particles, the zero-banana-orbit width, the large-aspect-ratio approximation, or the simplified collisionality. The highlight of the extended POCA simulations that include $\vec{E} \times \vec{B}$ is the clear verification of the BH resonances by periodically closed orbits, which can be understood as modified banana orbits effectively without the $\vec{E} \times \vec{B}$ precession drift.

Figure 1 shows typical examples for a modified banana orbit of a particle by the fast $\vec{E} \times \vec{B}$ drift motion (Red), compared to the original banana motion without $\vec{E} \times \vec{B}$ (Blue). Figure 1(a) is for $(\ell, n) = (1, 1)$ with $\epsilon = 0.25$ and Fig. 1(b) is for $(\ell, n) = (1, 3)$ with $\epsilon = 0.5$, where ϵ is the inverse aspect ratio. Here, the magnetic drift motion will be ignored for a moment for simplification. Both orbits are effectively not moving through periods, although one case (Red) includes the fast $\vec{E} \times \vec{B}$ precession. One can see from the Red trajectories in Fig. 1 that the toroidal motion is fast when the particle moves up from the lower to the upper turning point and is slow when the particle moves down, since the parallel bounce motion and perpendicular $\vec{E} \times \vec{B}$ drift can be added or subtracted for the toroidal motion. In both cases, the particle can radially drift out fast with a nonaxisymmetric perturbation, due to the absence of phase-mixing effects. When a magnetic perturbation is applied, a particle can drift off the magnetic surface since the action $J = \oint M v_\parallel dl$ can no longer be conserved within the surface. The radial drift can be random, but will be rapidly increased to one direction when orbits are nearly closed.

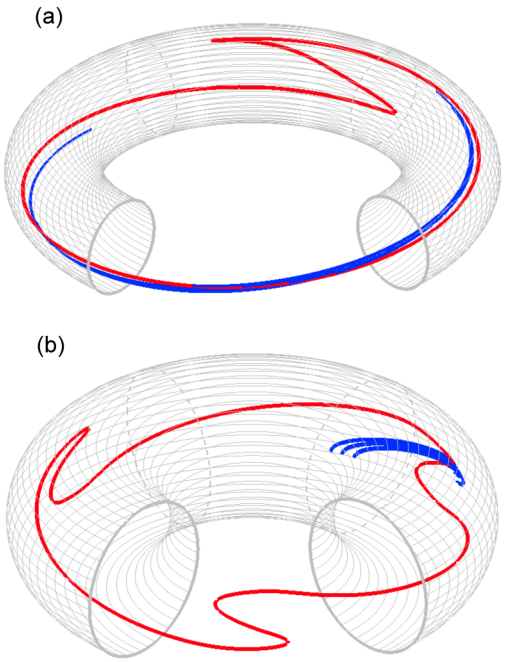

FIG. 1 (color online). 3D particle trajectories of the closed orbit with $\vec{E} \times \vec{B}$ (Red) compared to the original banana orbit without $\vec{E} \times \vec{B}$ (Blue) in the nonaxisymmetric configurations for (a) $(\ell, n) = (1, 1)$ and (b) $(\ell, n) = (1, 3)$. The closed orbit of the ℓ-class particle toroidally circulates ℓ cycles for n bounces as shown.

The increase of the radial drift by closed orbits is clearly illustrated in Fig. 2, where particle trajectories at near-zero precession, off resonances, and near resonance are shown for the same time interval. Here, collisions are not introduced for better graphical illustration, and a magnetic perturbation $(m, n) = (7, 3)$ with the poloidal mode number m is applied to produce the radial drift in the absence of collisions. The large radial drift can be seen by the $\omega_E \sim 0$ case in Fig. 2, as orbits are nearly closed without the precession, often called the superbanana plateau resonance [16]. As ω_E is increased $(3\omega_E < \omega_b)$, one can see the decrease of the radial drift, which is due to the random phase mixing. When ω_E approaches the first BH resonant frequency $(3\omega_E \sim \omega_b)$, the radial drift increases since the phase mixing is not effective with closed orbits. If ω_E is further increased $(3\omega_E > \omega_b)$, the drift decreases since the phase mixing takes effects again. Note here that the radial drifts are enhanced actually by nearly closed orbits, not by

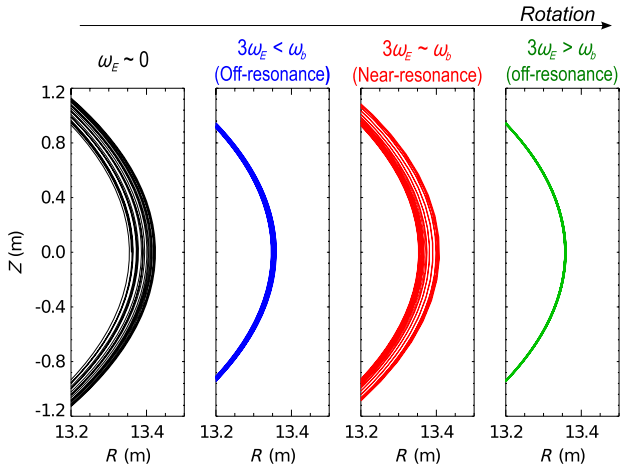

FIG. 2 (color online). Projections of particle orbits on the poloidal cross section at near-zero, off-resonant, and near-resonant precessions. Particles radially drift fast at the near-zero precession (superbanana plateau—Black) and at the near-resonant precession (BH resonance—Red), while the drifts are decreased at the off-resonant precessions (Blue, Green) due to the random phase mixing.

perfectly closed orbits, as the slight toroidal reposition of orbits is needed for orbit evolutions through different $|B|$. However, there is no distinction for the effects in the presence of collisions, which can move the closed orbits to different toroidal positions as the slight off-resonant $\vec{E}\times\vec{B}$ does.

Another important aspect in the BH resonances is the modification of the resonant magnetic perturbation. It is often believed that the NTV is driven by nonresonant magnetic perturbation, but the NTV transport is the largest when the magnetic perturbation satisfies the resonant condition $m - nq = 0$ with safety factor q, as described in detail by Kim *et al.* [21]. The resonant condition actually means that the wave front of the magnetic perturbation is the same as the helical pitch of the equilibrium magnetic field, or equivalently the path of the bounce orbits without the $\vec{E}\times\vec{B}$ precession, the blue trajectories in Fig. 1. When the bounce orbits are modified by the $\vec{E}\times\vec{B}$ precession, the wave front of the resonant perturbation should also be shifted to follow the path of the modified bounce orbits, the red trajectories in Fig. 1. This is predicted by theory with the condition $m - nq \pm \ell = 0$. Magnetic perturbations in Figs. 1 and 2 are actually chosen to meet the shifted resonant condition. For Fig. 1(a), the $(m, n) = (3, 1)$ perturbation is applied on the $q = 4$ surface, and for Figs. 1(b) and 2, the $(m, n) = (7, 3)$ perturbation is applied on the $q = 8/3$ surface to produce the $\ell = 1$ BH resonances. If a nonresonant perturbation is applied, for instance $(m, n) = (8, 3)$ to a $q = 8/3$ surface, each of three periods will experience different perturbations, and thus, the resonant enhancement can be largely decreased even though the orbits will repeat after three periods.

The described nature has been previously predicted by analytic theory, but the study with the POCA code verifies the existence and essential feature of the BH resonances. The theory can be summarized by an analytic NTV formula, which is given as

$$\tau_\varphi = \frac{\epsilon^{1/2} p}{\sqrt{2}\pi^{3/2} R_0} \int_0^\infty dx R_{1\ell} \int_0^1 d\kappa^2 \delta^2_{w\ell} \left[\omega_\varphi - \omega_{\rm nc}\right], \quad (1)$$

where

$$\delta^2_{w\ell} = \sum_{nmm'} \delta^2_{nmm'} \frac{F^{-1/2}_{nm\ell} F^{-1/2}_{nm'\ell}}{4K(\kappa)},$$

$$R_{1\ell} = \frac{1}{2} \frac{n^2\left[1 + \left(\frac{\ell}{2}\right)^2\right]^{\frac{\nu}{2\epsilon}} x e^{-x}}{(\ell\omega_b - n\omega_E - n\omega_B)^2 + \left\{\left[1 + \left(\frac{\ell}{2}\right)^2\right]^{\frac{\nu}{2\epsilon}} x^{-3}\right\}^2},$$

with p the pressure and R_0 the major radius. Here, normalized variables $x \equiv E/T$ and $\kappa^2 \equiv [E - \mu B_0(1-\epsilon)]/2\mu B_0\epsilon$ are used with kinetic energy E, temperature T, and magnetic moment μ. Given a magnetic field model $B = B_0(1 - \epsilon\cos\vartheta) + B_0\sum_{nm}\delta_{nm}e^{i(m\vartheta - n\varphi)}$ with B_0 the toroidal magnetic field at the magnetic axis, $\delta^2_{nmm'} \equiv \mathrm{Re}(\delta_{nm})\mathrm{Re}(\delta_{nm'}) + \mathrm{Im}(\delta_{nm})\mathrm{Im}(\delta_{nm'})$, $F^y_{nml}(\kappa) = \int_{-\vartheta_t}^{\vartheta_t} d\vartheta[\kappa^2 - \sin^2(\vartheta/2)]^y \cos[\Theta_{nm\ell}(\vartheta)]$ with $\Theta_{nm\ell} \approx (m - nq \pm \ell)\vartheta$ and $\vartheta_t = 2\arcsin(\kappa)$, and K is the complete elliptic integral of the first kind. The resonant precession condition is represented by $(\ell\omega_b - n\omega_E - n\omega_B)^2$ in the denominator of $R_{1\ell}$ in the first integral, and the resonant field condition can be found by the fact that $\delta^2_{w\ell}$ in the second integral is the largest when $m - nq \pm \ell = 0$. The last term represents the effect of neoclassical offset rotation $\omega_{\rm nc}$ [11]. See Ref. [17] for more details. This combined NTV theory presently gives the NTV torque by the BH resonances uniquely, so the formula was used for a quantitative comparison of BH resonant frequency and NTV with the POCA simulation.

The POCA solves a set of Hamiltonian orbit equations for the toroidal flux ψ, the poloidal angle ϑ, the toroidal angle φ, and the parallel gyroradius $\rho_\parallel = Mv_\parallel/qB$ [21,22]. It tracks the guiding-center orbit motion by solving the equations of motion in Boozer coordinates. Then, POCA calculates the neoclassical transport from the Fokker-Planck equation with δf Monte Carlo method [23]. Noting the distribution function f can be approximated as $f = f_M + \delta f = f_M \exp(\hat{f}) \approx f_M(1 + \hat{f})$ in the fusion plasmas with f_M the local Maxwellian, δf the perturbed distribution function, and $\hat{f}$ the deviation from Maxwellian, the Fokker Planck equation is written as

$$\frac{d\ln f_M}{dt} + \frac{d\hat{f}}{dt} = C_m, \quad (2)$$

where $C_m = C/f$ and C is the collision operator. Eq. (2) is rewritten as

$$\frac{d\hat{f}}{dt} = -\vec{v}\cdot\vec{\nabla}\psi \frac{\partial \ln f_M}{\partial\psi} + C_m, \quad (3)$$

and $\hat{f}$ is obtained from following equation,

$$\Delta\hat{f} = -\Delta\psi \frac{\partial \ln f_M}{\partial\psi} + 2\nu\frac{u}{v}\lambda\Delta t - \Delta\psi\frac{e}{T}\frac{d\Phi}{d\psi}, \quad (4)$$

with ν the collision frequency, u the parallel flow velocity, λ the pitch angle, and e the electric charge. A modified pitch-angle scattering collision operator is employed using a Monte Carlo equivalent of the pitch-angle collision operator [24] which updates λ by pitch-angle scattering, and a momentum correction term [23,25] is added to the collision operator for conserving the toroidal momentum. The first term in the right hand side of Eq. (4) represents δf driven by particle drift motions, and the second term by the toroidal momentum conservation. The third term represents the effect of electric potential Φ, which is directly related to $\vec{E}\times\vec{B}$ rotation and the electric precession by radial electric field $E_r = -d\Phi/dr$. Finally, the POCA code estimates the NTV torque by calculating the perturbed pressures and utilizing the magnetic field spectrums as $\tau_\varphi = \langle \mathbf{e}_\varphi \cdot \nabla \cdot \mathbf{P}\rangle = \langle \delta P/B \cdot \partial B/\partial\varphi\rangle$ with

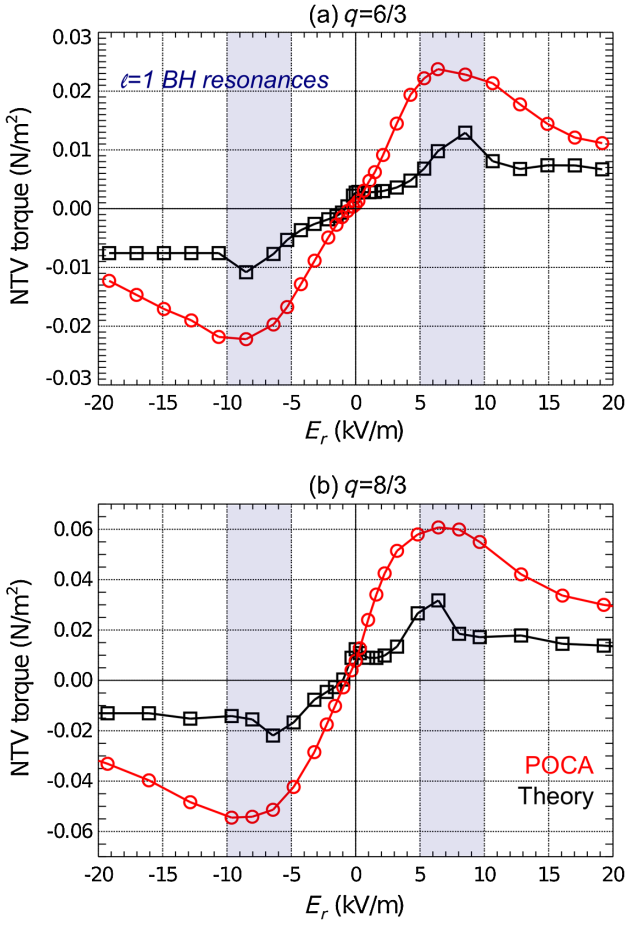

FIG. 3 (color online). NTV torque scan as a function of radial electric field at (a) $q = 6/3$ surface and (b) $q = 8/3$ surface, where BH resonances appear for $n = 3$ perturbations and $\ell = 1$ class particles. NTV peaks by the BH resonances are clearly found around the predicted resonant E_r.

$\mathbf{e}_\varphi = \partial \mathbf{x}/\partial \boldsymbol{\varphi}$ [26]. δP is the perturbed pressure defined by $\delta P = \int d^3v (M v_\perp^2/2 + M v_\parallel^2)\delta f$, and brackets denote the flux surface average. In this Letter, we apply an analytic nonaxisymmetric field perturbation expressed as $\delta B/B_0 = \delta_{mn}(\psi_n)\cos(m\vartheta - n\varphi)$ with ψ_n the normalized poloidal flux, then the NTV torque is calculated by

$$\tau_\varphi = B_0 n \delta_{mn} \left\langle \frac{\delta P}{B} \sin(m\vartheta - n\varphi) \right\rangle. \quad (5)$$

For quantitative comparison of the NTV torque, an example is set by a single harmonic perturbation with $\delta_{mn} = 0.02\psi_n^2$ and $(m, n) = (7, 3)$ to a model plasma in Ref. [21], where $T_{i,0} = 500$ eV, $B_0 = 10$ T, $R_0 = 10$ m, $a = 2.5$ m, $q_0 = 1.2$, $q_{\text{edge}} = 11.0$, and $\nu_* \sim 1.0$. The NTV torque is calculated by scanning the electric precession frequency. According to the combined NTV theory, the BH resonances should occur at $\omega_E \sim \omega_b/3$ for $n = 3$ perturbations and $\ell = 1$ class particles, where $E_r \sim \pm 7$ kV/m for the model plasma. Figure 3 shows the NTV torques as a function of radial electric field E_r at $q = 6/3$ and $q = 8/3$ surfaces, where $\ell = 1$ class particles satisfy the resonant field condition $m - nq \pm \ell = 0$ with the applied perturbations.

In Fig. 3, both POCA and theory calculations indicate clear NTV peaks enhanced by the BH resonances. The resonant $\vec{E} \times \vec{B}$ frequency for the peak NTV by the POCA simulation is consistent with the theory prediction, indicating the importance of BH resonances. The amplitudes of NTV agree within a factor of 2 or 3. The NTV peaks appear broad, since ω_b and ω_E are continuous functions of plasma parameters and there is a small fraction of resonant particles of $\ell > 1$. It is notable that the enhanced NTV can be even stronger than the theoretically predicted value. It may be largely due to finite-orbit-width and passing particle effects, which are excluded in the combined theory. These effects are obviously more important when the $\vec{E} \times \vec{B}$ rotation is stronger, as the POCA simulation largely improved the prediction on NTV in the magnetic braking experiments for NSTX with fast precession and large orbit width [27]. Note that the BH resonances can occur at every flux surface since the nonaxisymmetric magnetic perturbations are composed of a multiharmonic Fourier series, of which a certain component can meet the resonant field condition at the surface. Also, there is always a fraction of particles with low energy and bounce frequency in a Maxwellian distribution. These particles can resonate even with the low $\vec{E} \times \vec{B}$ precession, and thus, enhance the NTV.

In summary, this POCA simulation verifies the bounce-harmonic resonance and its crucial role in NTV physics. It is clearly shown that the electric precession modifies a banana orbit to a new type of closed orbit, and significantly enhances the particle transport by preventing the phase mixing when the precession frequency becomes resonant. As a result, the bounce-harmonic resonances can greatly enhance the NTV torque. This Letter shows that the bounce harmonic resonance is the critical physics driving NTV in the finite $\vec{E} \times \vec{B}$ rotation, and thus, should be understood for reliable prediction of particle transport and NTV in the present tokamaks and International Thermonuclear Experimental Reactor.

K. K. would like to thank Walter Guttenfelder for useful comments. This work was supported by DOE Contract No. DE-AC02-09CH11466.

*kkim@pppl.gov

[1] T. E. Evans, R. A. Moyer, P. R. Thomas, J. G. Watkins, T. H. Osborne, J. A. Boedo, E. J. Doyle, M. E. Fenstermacher, K. H. Finken, R. J. Groebner, *et al.*, Phys. Rev. Lett. **92**, 235003 (2004).

[2] S. A. Sabbagh, R. E. Bell, J. E. Menard, D. A. Gates, A. C. Sontag, J. M. Bialek, B. P. LeBlanc, F. M. Levinton, K. Tritz, and H. Yuh, Phys. Rev. Lett. **97**, 045004 (2006).

[3] W. Suttrop, T. Eich, J. C. Fuchs, S. Günter, A. Janzer, A. Herrmann, A. Kallenbach, P. T. Lang, T. Lunt, M. Maraschek, *et al.*, Phys. Rev. Lett. **106**, 225004 (2011).
[4] Y. M. Jeon, J.-K. Park, S. W. Yoon, W. H. Ko, S. G. Lee, K. D. Lee, G. S. Yun, Y. U. Nam, W. C. Kim, J.-G. Kwak *et al.*, Phys. Rev. Lett. **109**, 035004 (2012).
[5] A. H. Boozer, Phys. Rev. Lett. **86**, 5059 (2001).
[6] A. J. Cole, C. C. Hegna, and J. D. Callen, Phys. Rev. Lett. **99**, 065001 (2007).
[7] J. D. Callen, A. J. Cole, and C. C. Hegna, Nucl. Fusion **49**, 085021 (2009).
[8] J.-K. Park, A. H. Boozer, J. E. Menard, A. M. Garofalo, M. J. Schaffer, R. J. Hawryluk, S. M. Kaye, S. P. Gerhardt, and S. A. Sabbagh (NSTX Team), Phys. Plasmas **16**, 056115 (2009).
[9] S. A. Sabbagh, J. W. Berkery, R. E. Bell, J. M. Bialek, S. P. Gerhardt, J. E. Menard, R. Betti, D. A. Gates, B. Hu, O. N. Katsuro-Hopkins *et al.*, Nucl. Fusion **50**, 025020 (2010).
[10] S. P. Gerhardt, J. E. Menard, J.-K. Park, R. Bell, D. A. Gates, B. P. L. Blanc, S. A. Sabbagh, and H. Yuh, Plasma Phys. Controlled Fusion **52**, 104003 (2010).
[11] A. M. Garofalo, K. H. Burrell, J. C. DeBoo, J. S. deGrassie, G. L. Jackson, M. Lanctot, H. Reimerdes, M. J. Schaffer, W. M. Solomon, and E. J. Strait, Phys. Rev. Lett. **101**, 195005 (2008).
[12] H. Reimerdes, A. M. Garofalo, E. J. Strait, R. J. Buttery, M. S. Chu, Y. In, G. L. Jackson, R. J. L. Haye, M. J. Lanctot, Y. Q. Liu *et al.*, Nucl. Fusion **49**, 115001 (2009).
[13] K. C. Shaing, Phys. Plasmas **10**, 1443 (2003).
[14] K. C. Shaing, P. Cahyna, M. Becoulet, J.-K. Park, S. A. Sabbagh, and M. S. Chu, Phys. Plasmas **15**, 082506 (2008).
[15] X. Garbet, J. Abiteboul, E. Trier, Ö. Gürcan, Y. Sarazin, A. Smolyakov, S. Allfrey, C. Bourdelle, C. Fenzi, V. Grandgirard *et al.*, Phys. Plasmas **17**, 072505 (2010).
[16] A. J. Cole, J. D. Callen, W. M. Solomon, A. M. Garofalo, C. C. Hegna, M. J. Lanctot, H. Reimerdes, and the DIII-D Team, Phys. Rev. Lett. **106**, 225002 (2011).
[17] J.-K. Park, A. H. Boozer, and J. E. Menard, Phys. Rev. Lett. **102**, 065002 (2009).
[18] K. C. Shaing, S. A. Sabbagh, and M. S. Chu, Nucl. Fusion **50**, 025022 (2010).
[19] R. Linsker and A. H. Boozer, Phys. Fluids **25**, 143 (1982).
[20] H. E. Mynick, Nucl. Fusion **26**, 491 (1986).
[21] K. Kim, J.-K. Park, G. J. Kramer, and A. H. Boozer, Phys. Plasmas **19**, 082503 (2012).
[22] R. B. White, Phys. Fluids B **2**, 845 (1990).
[23] M. Sasinowski and A. H. Boozer, Phys. Plasmas **4**, 3509 (1997).
[24] A. H. Boozer and G. Kuo-Petravic, Phys. Fluids **24**, 851 (1981).
[25] M. N. Rosenbluth, R. D. Hazeltine, and F. L. Hinton, Phys. Fluids **15**, 116 (1972).
[26] J. D. Williams and A. H. Boozer, Phys. Plasmas **10**, 103 (2003).
[27] K. Kim, J.-K. Park, G. J. Kramer, A. H. Boozer, J. E. Menard, S. P. Gerhardt, and NSTX Team, in *Proceedings of 24th IAEA Fusion Energy Conference* (IAEA, San Diego, 2012).